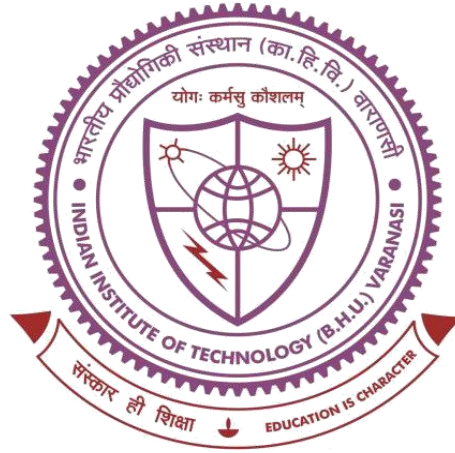


BOVINE MILK EXOSOMES FOR THE TREATMENT OF MELANOMA



Thesis submitted in partial fulfillment for the
Award of Degree

Doctor of Philosophy

By

Dulla Naveen Kumar

DEPARTMENT OF PHARMACEUTICAL ENGINEERING & TECHNOLOGY
INDIAN INSTITUTE OF TECHNOLOGY (BHU) VARANASI
VARANASI – 221005
INDIA

Roll No- 20161506

Year 2024



Dedicated

To

Nation

CERTIFICATE

It is certified that the work contained in the thesis titled "*Bovine milk exosomes for the treatment of melanoma*" by *Mr. Dulla Naveen Kumar* has been carried out under my supervision and that this work has not been submitted elsewhere for a degree.

It is further certified that the student has fulfilled all the requirements of Comprehensive Examination, Candidacy and SOTA for the award of Ph.D. degree.

Ashish K. Agrawal
10/12/2024

Dr. Ashish Kumar Agrawal

Supervisor

आशीष कु० अग्रवाल / Ashish K. Agrawal
सह आचार्य / Associate Professor
भैषजकीय अभियांत्रिकी एवं प्रौद्योगिकी विभाग /
Department of Pharmaceutical Engineering & Technology
भारतीय प्रौद्योगिकी संस्थान / Indian Institute of Technology
(काशी हिन्दू विश्वविद्यालय) / (Banaras Hindu University)
वाराणसी-२२१००५ / Varanasi-221005
E-mail: ashish.phe@iitbhu.ac.in

DECLARATION BY THE CANDIDATE

I, "**Dulla Naveen Kumar**", certify that the work embodied in this thesis is my own bonafide work and carried out by me under the supervision of "**Dr. Ashish Kumar Agrawal**" from "**January 2021**" to "**December 2024**", at the "**Department of Pharmaceutical Engineering & Technology**", Indian Institute of Technology (BHU), Varanasi. The matter embodied in this thesis has not been submitted for the award of any other degree/diploma. I declare that I have faithfully acknowledged and given credits to the research workers wherever their works have been cited in my work in this thesis. I further declare that I have not willfully copied any other's work, paragraphs, text, data, results, etc., reported in journals, books, magazines, reports dissertations, theses, etc., or available at websites and have not included them in this thesis and have not cited as my own work.

Date: 10.12.2024


Place: Varanasi


Dulla Naveen Kumar

CERTIFICATE BY THE SUPERVISOR

It is certified that the above statement made by the student is correct to the best of my knowledge.


Dr. Ashish Kumar Agrawal
Supervisor
आशीष कु० अग्रवाल / Ashish K. Agrawal
सह आचार्य / Associate Professor
भैषजकीय अभियांत्रिकी एवं प्रौद्योगिकी विभाग /
Department of Pharmaceutical Engineering & Technology
भारतीय प्रौद्योगिकी संस्थान / Indian Institute of Technology
(काशी हिन्दू विश्वविद्यालय) / (Banaras Hindu University)
वाराणसी-२२१००५ / Varanasi-221005
E-mail: ashish.phe@iitbhu.ac.in


Head of the Department
विभागाध्यक्ष / Head
भैषजकीय अभियांत्रिकी एवं प्रौद्योगिकी विभाग /
Department of Pharmaceutical Engineering & Technology
भारतीय प्रौद्योगिकी संस्थान / INDIAN INSTITUTE OF TECHNOLOGY
(बनारस हिन्दू विश्वविद्यालय) / (BANARAS HINDU UNIVERSITY)
वाराणसी-२२१००५ / Varanasi-221005

COPYRIGHT TRANSFER CERTIFICATE

Title of the Thesis: Bovine milk exosomes for the treatment of melanoma

Name of the Student: Dulla Naveen Kumar

COPYRIGHT TRANSFER

The undersigned hereby assigns to the Indian Institute of Technology (Banaras Hindu University), Varanasi, all rights under copyright that may exist in and for the above thesis submitted for the award of the "*Doctor of Philosophy*".

Date: 10.12.2024

Place: Varanasi


Dulla Naveen Kumar

ACKNOWLEDGEMENT

*With humility, misty eyes, and folded hands, I sincerely acknowledge my gratitude to the Almighty for showering his blessings upon me. I would like to thank the God of wisdom, knowledge, and prosperity “**Lord Ganesha Ji,**” Deva Deva Mahadeva “**Kashi Vishwanath Ji,**” Lord of the Universe “**Lord Jagannath Ji**” for showering their continuous blessings. The Almighty constantly infused me with the strength and concentration to embark on and accomplish this work successfully. This research work would not be possible without their benediction and grace. I pray that this hidden force always blesses me with the strength, courage, wisdom, and willpower to face all the challenges of life.*

My first and foremost heartfelt gratitude and indebtedness would be towards “**Bharat Ratna Mahamana Pandit Madan Mohan Malviya Ji,**” the founder of Banaras Hindu University, for establishing a magnificent temple of learning. I am extremely grateful to “**Prof. Mahadeva Lal Schroff,**” the father of Indian pharmacy education, for his great contributions to the field of pharmacy towards the introduction of Bachelor's and Master Degree courses in the Discipline of Pharmaceutical Sciences in India.

*I would like to express a deep sense of gratitude, appreciation, and indebtedness to my honourable supervisor **Dr. Ashish Kumar Agrawal,** for providing his continuous support, motivation, and immense knowledge towards the conceptualization, experiment designing, project investigation, supervision, data interpretation, expert assistance, editing, drafting, and revision functions. His professional acumen, plausible and erudite thinking, and perfect counseling helped me in achieving my goal. His meticulous ways, utmost attention to all problems, continuous involvement, precious guidance, valued suggestions, and tireless efforts made this immense task come to a conclusion successfully. I am also thankful to him for providing the necessary facilities to carry out this research work. I feel fortunate to have been associated with and worked under such an accomplished personality.*

*I would also like to thank my Research Progress Evaluation Committee (RPEC) members, **Dr. Dinesh Kumar** (Assistant Professor, Department of Pharmaceutical Engineering and Technology, IIT (BHU), Varanasi) and **Dr. Vishal Mishra** (Assistant Professor, School of Biochemical Engineering, IIT (BHU), Varanasi) for their valuable guidance, supervision, expert assistance, scientific inputs, and suggestions throughout the experiments.*

*I express my gratitude to **Prof. Siva Hemalatha**, Head, Department of Pharmaceutical Engineering & Technology, I.I.T. (B.H.U.), Varanasi, for providing the necessary facilities and academic guidance during my Ph.D. work. I am immensely thankful to all former Head of the Department, **Prof. Brahmeshwar Mishra**, **Prof. Sushil Kumar Singh**, **Prof. Sanjay Singh**, and **Prof. Sushant Kumar Shrivastava**, for their cooperation during my research work.*

*I express my gratitude to all the faculty members and scientific officer of the Department of Pharmaceutical Engineering & Technology: **Prof. Sairam Krishnamurthy**, **Prof. Senthil Raja A.**, **Dr. Ruchi Chawla**, **Prof. M. S. Muthu**, **Dr. Sunil K Mishra**, **Dr. Prasanta K. Nayak**, **Dr. Gyan Prakash Modi**, **Dr. Vinod Tiwari**, **Dr. Alakh N Sahu**, **Dr. Rajnish**, **Dr. Deepak Kumar**, **Dr. Dinesh Kumar**, **Dr. Jairam Meena**, **Dr. Ashok Kumar**, and **Dr. Arun Khatri** for their cooperation, and scientific suggestions during my research work. My access to their Laboratory for various works during my Ph.D. works is highly acknowledged. Without their precious support, it would not have been possible to execute this research work.*

*My sincere thanks to **Dr. Armin Gamper** (Associate professor, Department of Oncology, Cross Cancer Institute, University of Alberta, Edmonton, Canada) for allowing me to work with him and for valuable research suggestions during my SERB-OVDF program.*

*My heartiest thanks to my lab mates at the nanomedicine Research laboratory: **Ms. Aiswarya Chaudhuri**, **Dr. Deepa Dehari**, **Mr. Korra Remesh**, **Mr. Rohit Patil**, **Ms. Komal Rani**, **Ms. Udita Shiromani**, **Mr. Sourav Bera**, **Mr. Sanchit Arora**, and **Mr. Rohan Sahu**, for making wonderful friendly environment in lab which made my work fruitful and enjoyable. They always had a friendly attitude and, at the same time, provided me with valuable suggestions, which helped me in carrying out my research work.*

*I am thankful to **Dr. A N Sahu**, **Dr. Debadatta Mohapatra**, **Dr. Subash Chandra Gupta**, **Dr. Geeta Rai** (Assistant professor, BHU), **Dr. Kushbhu Priya**, **Ms. Anusmita**, **Mr. Ankit Srivastava**, and **Dr. Ramakrishna Kakarla** for their collaborative work.*

*My thankful regards to my batch mates, friends and seniors **Dr. Harish Indurthi**, **Mr. Anoop Kumar Tiwari**, **Dr. Samarпита Das**, **Mr. Obulapathi**, **Mr. Venkateshwarlu**, **Mr. Anurag**, **Mr. Bhanuranjan** and **Mr. Himanshu Rai**, **Dr. Singh Shreya**, **Dr. Digambar** and **Ms. Pallavi Saha** for their pleasant company, cooperation, and help during research work.*

*Finally, I shall always remain thankful and indebted to my parents, **Mr. Dulla Buddaiah** and **Mrs. Dulla Sugunamma**, my fiancée **Meghana A** (Chikka Dean) and my brother **Mr. Praveen***

(Mittu), and family members Mr. Varukolu Suresh, Mrs. Varukolu Sravani, Neha Gupta, Siddu, Satish, and Mallesh for all their selflessly sacrifices, love, support, strength, and cooperation during the study. This work could not have been completed without their blessings. I have no words to thank them all.

*Last but not least, I am grateful and would like to **thank everybody** who some or the other who contributed to this research work and motivated me to overcome hurdles during this journey.*

*The financial assistance for this work provided as a scholarship to me by the **Science and Engineering Research Board (SERB) and Ministry of Human Resource Development (MHRD)**, Government of India, is highly acknowledged. I greatly acknowledge the **Central Instrumentation Facility at IIT (BHU), Varanasi**, for providing the facility for various analysis.*

*I am very much thankful to the **instrumental and infrastructure facilities** provided by the **Department of Pharmaceutical Engineering & Technology, IIT (BHU), Varanasi; Central Instrument Facility, IIT (BHU), Varanasi, India.***



Date: 16-12-2024

Place: Varanasi

Dulla Naveen Kumar

List of Figures

Figure 2.1 Anatomy of the skin, showing the epidermis, dermis, and subcutaneous tissue. Melanocytes are in the layer of basal cells at the deepest part of the epidermis.	9
Figure 2.2 Expected cases and expected mortalities of melanoma in the US by 2023.....	10
Figure 2.3 Graphical representation of melanomas with characteristic asymmetry, border irregularity, color variation, and large diameter (ABCD).....	12
Figure 2.4 Graphical representation of the progression of melanoma.	13
Figure 2.5 Graphical representation of types of melanomas.	13
Figure 2.6 Mitogen-activated protein kinase (MAPK pathway) and phosphoinositide-3-OH kinase (PI3K/Akt).	16
Figure 2.7 Immune checkpoint inhibitor. Checkpoint proteins, such as B7-1/B7-2 on antigen-presenting cells (APC) and CTLA-4 on T cells, help keep the body's immune responses in check. When the T-cell receptor (TCR) binds to the antigen and major histocompatibility complex (MHC) proteins on the APC and CD28 binds to B7-1/B7-2 on the APC, the T cell can be activated.....	18
Figure 2.8 Graphical representation of the use of natural products in cancer treatment.	23
Figure 2.9 Structure of dihydroartemisinin.....	25
Figure 2.10 Structure of Hesperidin.....	30
Figure 2.11 Graphical representations of the mechanism of actions of DHA and HES in cancer.	32
Figure 2.12 Graphical structure of exosomes.	34
Figure 2.13 Graphical representation of advantages of exosomes compared to other drug delivery systems.....	36
Figure 2.14 Graphical representation of biogenesis of exosomes.	37
Figure 2.15 Schematic diagram showing different methods of loading cargos into exosomes through pre-loading and post-loading strategies: (A) incubation with parent cell; (B) incubation; (C) sonication; (D) electroporation; (E) detergent method; (F) excursion; (G) freeze-thaw cycle.	41
Figure 5.1 Graphical representation of the flow of work for Chapter 5.	55
Figure 5.2 Schematic diagram of isolation of exosomes from bovine milk.	61
Figure 5.3 Graphical representation of the procedure for colony formation assay.....	69
Figure 5.4 Graphical representation of <i>in vitro</i> transwell migration assay.	70
Figure 5.5 Graphical representation of wound healing assay.	70
Figure 5.6 Graphical representation of tumor model development and treatments in Swiss mice.....	73
Figure 5.7 Graphical representation for the model development of pulmonary metastasis and treatment in Swiss mice.	75
Figure 5.8 The HPLC and DAD signal chromatograms of DHA at wavelength 266 nm, mobile phase methanol: water (80:20).....	76
Figure 5.9 HPLC-based calibration curve of DHA measured at 266 nm.	76
Figure 5.10 (A) HPLC and DAD signal chromatograms of DHA in plasma and (B) blank plasma at wavelength 266 nm, mobile phase methanol: water (80:20).....	79
Figure 5.11 HPLC-based calibration curve of DHA in plasma measured at 266 nm.	80
Figure 5.12 Exosomes were isolated in three batches via ultracentrifugation, and purity was confirmed via exosomal and microvesicle biomarkers.....	82

Figure 5.13 Morphology, size, and zeta potential of exosomes and DHA-loaded exosomes: (A-C) Morphology by SEM, AFM, and Size by particle size analyzer of exosomes; (D-E) Morphology by SEM, AFM, and Size by particle size analyzer of Exo-DHA.....	84
Figure 5.14 3D response surface plots indicating the interaction of the independent variables on particle size (A-C), PDI (D – F), % encapsulation efficiency (G – I), and % drug loading (J – L).....	86
Figure 5.15 Residual plots showing the run distribution for particle size (A), PDI (B), % encapsulation efficiency (C), and % drug loading (D).	87
Figure 5.16 XRD and stability of Exo and Exo-DHA, (A) represent XRD of Exo, DHA, and Exo-DHA, (B) stability of exosomes when stored in refrigerated conditions for different times in terms of the effect on (I) particle size, (II) PDI, (III) zeta potential.	88
Figure 5.17 Drug release for DHA and Exo-DHA was performed at pH 7.4 (A) and pH 5.5 (B) via the dialysis bag method. pH 7.4 mimics the blood condition, and pH 5.5 mimics the tumor environment.....	90
Figure 5.18 Cytotoxicity of DHA and Exo-DHA in (I) B16F10 cell lines, and (II) HEK-293 cell lines for 24, 48, and 72 h. Statistical analysis was performed by One-Way ANOVA followed by the Tukey P test with multiple comparisons and the level of significance * $p < 0.05$, ** $p < 0.01$, and *** $p < 0.001$	90
Figure 5.19 Qualitative cellular uptake of Coumarin-6 and Coumarin-6 loaded exosomes in B16F10 cell lines. Cells were observed in the green channel for C-6 and the blue channel for DAPI. Statistical analysis was performed by One-Way ANOVA followed by the Tukey P test with multiple comparisons and the level of significance * $p < 0.05$	91
Figure 5.20 Nuclear DNA fragmentation assay performed with DAPI staining.	92
Figure 5.21 Apoptosis assay was performed by acridine orange/ethidium bromide in B16F10 cell lines. Acridine orange binds to the live cells, while ethidium bromide binds to the dead cells. AI: Indicates the apoptotic index.	93
Figure 5.22 Reactive oxygen species assay by flow cytometry (A), and fluorescence microscopy (B). After the treatment cells were incubated with H2DCFDA dye. Statistical analysis was performed by One-Way ANOVA followed by the Tukey P test with multiple comparisons and the level of significance ** $p < 0.01$ and *** $p < 0.001$	94
Figure 5.23 Mitochondrial membrane potential assay, green fluorescence indicates JC-1 monomers and red fluorescence indicates the J-aggregates. Statistical analysis was performed by One-Way ANOVA followed by the Tukey P test with multiple comparisons and the level of significance ** $p < 0.01$ and *** $p < 0.001$	96
Figure 5.24 Colony formation assay was performed in B16F10 cell lines. Treatment was given with exosomes, DHA, and Exo-DHA. Statistical analysis was performed by One-Way ANOVA followed by the Tukey P test with multiple comparisons and the level of significance * $p < 0.05$, ** $p < 0.01$ and *** $p < 0.001$	97
Figure 5.25 Transwell migration assay shows the Exo-DHA significantly reduces the migration of B16F10 cell lines. (A) represents control, (B) treated with exosomes, (C) treated with DHA, (D) treated with Exo-DHA. Statistical analysis was performed by One-Way ANOVA followed by the Tukey P test with multiple comparisons and the level of significance * $p < 0.05$, ** $p < 0.01$	98
Figure 5.26 Wound healing assay was performed in B16F10 cell lines and healing was observed at 0, 12, and 24 h. Exo-DHA significantly inhibited the migration of the cells compared to DHA. The percent of wound healing is calculated via the (A) wound width with	

respect to time and (B) wound closure ($\mu\text{m}/\text{hour}$), (C) % of wound closure. Statistical analysis was performed by One-Way ANOVA followed by the Tukey P test with multiple comparisons and the level of significance * $p < 0.05$, ** $p < 0.01$ and *** $p < 0.001$	99
Figure 5.27 Improved anti-cancer efficacy of Exo-DHA <i>in vitro</i> was confirmed by western blotting by evaluating apoptotic, and migration proteins. The immune blotting was performed for Bcl-2, Bax, Survivine, and MMP-9. Statistical analysis was performed by One-Way ANOVA followed by the Tukey P test with multiple comparisons and the level of significance * $p < 0.05$, ** $p < 0.01$	100
Figure 5.28 Pharmacokinetic profile and tissue distribution of DHA and Exo-DHA after oral administration at 50 mg/kg. (A) represents the pharmacokinetic profile, and (B) tissue distribution. Statistical analysis was performed by One-Way ANOVA followed by the Tukey P test with multiple comparisons and the level of significance * $p < 0.05$, ** $p < 0.01$ and *** $p < 0.001$	102
Figure 5.29 <i>In vivo</i> DHA and Exo-DHA anti-cancer efficacy against B16F10 melanoma in Swiss albino mice. (A) representative images of animals at endpoint (day 28 of treatment), (B) representative tumors excised after euthanasia, (C) tumor growth kinetics, (D) percent tumor growth inhibition, (E) excised tumor weight, (F) body weight, (G) tumor volume doubling time, and (H) final tumor volume, Statistical analysis was conducted using One-Way ANOVA followed by the Tukey post hoc test for multiple comparisons. The significance levels were denoted as * $p < 0.05$, ** $p < 0.01$, and *** $p < 0.001$ to indicate the statistical significance of the results.....	104
Figure 5.30 Biochemical parameters (A) ALT, (B) AST, (C) ALP, (D) urea, (E) creatinine in plasma after the treatment. a: comparison with healthy, b: comparison with control, c: comparison with exosomes, d: comparison with Exo-DHA. Statistical analysis was performed by One-Way ANOVA followed by the Tukey P test with multiple comparisons and the level of significance * $p < 0.05$, ** $p < 0.01$, and *** $p < 0.001$	106
Figure 5.31 Histopathology of H&E stained vital organs isolated from tumor-bearing mice after the treatment. Arrows indicate signs of rupture in portal veins.....	108
Figure 5.32 An <i>in vivo</i> metastasis study was performed in Swiss mice. Exo-DHA significantly decreased the metastatic burden compared to DHA or DTIC treatment. Statistical analysis was performed by One-Way ANOVA followed by the Tukey P test with multiple comparisons and the level of significance * $p < 0.05$, ** $p < 0.01$, and *** $p < 0.001$	109
Figure 6.1 Graphical representation of the workflow for chapter 6.	113
Figure 6.2 The HPLC and DAD signal chromatograms of HES at wavelength 285 nm, mobile phase methanol: water (80:20).....	128
Figure 6.3 HPLC-based calibration curve of HES measured at 285 nm.	128
Figure 6.4 (A) HPLC and DAD signal chromatograms of HES in plasma and (B) blank plasma at wavelength 266 nm, mobile phase methanol: water (80:20).....	131
Figure 6.5 HPLC-based calibration curve of HES in plasma measured at 285 nm.....	132
Figure 6.6 Morphology of exosomes and Exo-HES: (A-B) Morphology by SEM, (C-D) morphology by AFM of Exo and Exo-HES, (E-F) size of Exo and Exo-HES via particle size analyzer, and (G) zeta potential.	135
Figure 6.7 XRD and drug release profile of exosomes, HES, and Exo-HES. (A) Represents XRD of exosomes, HES, Exo-HES, (B) Drug release profile at (I) pH 7.4 and (II) pH 5.5.	136
Figure 6.8 Cytotoxicity of HES and Exo-HES at different time points: (A) 24 h, (B) 48 h, (C) 72 h., and (D) IC50 values at different time points. Additionally, (E) depicts cell viability in	

HEK-293 cell lines, and (F) represents the IC ₅₀ values in tabular form. Statistical analysis was conducted using One-Way ANOVA, followed by the Tukey post hoc test for multiple comparisons. The significance levels are denoted as * <i>p</i> < 0.05, ** <i>p</i> < 0.01.	138
Figure 6.9 Qualitative cellular uptake of free coumarin-6 and coumarin-6 loaded exosomes in B16F10. Cells were observed in brightfield, the green channel for C-6, and the blue channel for DAPI.	139
Figure 6.10 Nuclear DNA fragmentation assay performed with DAPI staining.	140
Figure 6.11 The generation of reactive oxygen species was estimated via H ₂ DCFDA dye. (A) represents no treatment, (B) exosomes treated, (C) HES treated, (D) Exo-HES treated. (E) H ₂ O ₂ , (F) Fluorescence intensity. Statistical analysis was performed by One-Way ANOVA followed by the Tukey P test with multiple comparisons and the significance level * <i>p</i> < 0.05, ** <i>p</i> < 0.01, and *** <i>p</i> < 0.001.	141
Figure 6.12 In the mitochondrial membrane potential assay, green fluorescence indicates JC-1 monomers and red fluorescence indicates the J-aggregates. Statistical analysis was performed by One-Way ANOVA followed by the Tukey P test with multiple comparisons and the significance level ** <i>p</i> < 0.01, and *** <i>p</i> < 0.001.	143
Figure 6.13 Colony formation assay was performed in B16F10 cell lines. Treatment was given with exosomes, HES, and Exo-HES. Statistical analysis was performed by One-Way ANOVA followed by the Tukey P test with multiple comparisons and the significance level * <i>p</i> < 0.05 and *** <i>p</i> < 0.001.	144
Figure 6.14 Transwell migration assay shows the Exo-HES significantly reduces the migration of B16F10 cell lines. (A) represents control, (B) treated with exosomes, (C) treated with HES, (D) treated with Exo-HES, (E) number of migrated cells/field calculated via microscope. Statistical analysis was performed by One-Way ANOVA followed by the Tukey P test with multiple comparisons and the level of significance * <i>p</i> < 0.05, ** <i>p</i> < 0.01, and *** <i>p</i> < 0.001.	145
Figure 6.15 (A) Wound healing assay was performed in B16F10 cell lines, and healing was observed at 0 h, 12 h, and 24 h. The percent of wound healing is calculated via the (B-C) rate of the wound closure and (D) % of wound closure. Statistical analysis was performed by One-Way ANOVA followed by the Tukey P test with multiple comparisons and the level of significance * <i>p</i> < 0.05, ** <i>p</i> < 0.01, and *** <i>p</i> < 0.001.	146
Figure 6.16 Pharmacokinetic profile of HES and Exo-HES after oral administration at 25 mg/kg. (A-B) represents the pharmacokinetic profile and pharmacokinetic parameters in tabular form. Statistical analysis was performed by One-Way ANOVA followed by the Tukey P test with multiple comparisons and the level of significance ** <i>p</i> < 0.01 and *** <i>p</i> < 0.001. Values are represented as mean±SD.	148
Figure 6.17 Tumor images and tumor volumes of control, Exo, HES, Exo-HES, and DTIC-treated groups. (A) Final day tumors, (B) represents final-day tumors, (C) Tumor regression analysis representing the tumor volume in different treatment groups with respect to time, (D) Tumor weight, (E) tumor volume doubling time, (F) final tumor volume, (G) percent tumor growth inhibition, and (H) Body weight. Statistical analysis was performed by One-Way ANOVA followed by the Tukey P test with multiple comparisons and the level of significance * <i>p</i> < 0.05, ** <i>p</i> < 0.01, and *** <i>p</i> < 0.001.	149
Figure 6.18 Histopathology of different vital organs was performed by H&E staining. Organs were isolated from tumor-bearing mice after the treatment.	151

Figure 6.19 Assessment of biochemical parameters in plasma after treatment, including (A) ALT, (B) AST, (C) ALP, (D) Urea, and (E) Creatinine. Statistical analysis was conducted using One-Way ANOVA followed by the Tukey P test with multiple comparisons. The significance levels are indicated as $**p < 0.01$ 152

List of Tables

Drug repurposing offers several intrinsic advantages, including reduced development time and cost, owing to the pre-existing knowledge regarding the safety, dosage, and toxicity profiles of established drugs. Interest in this strategy has surged in recent years, with successful examples such as chlorambucil and bufalin, originally developed as alkylating agents based on the chemical warfare agent mustard gas, later proven effective for treating leukemias [113]. Additionally, thalidomide, despite its notorious history of severe teratogenic effects, has been repurposed for conditions such as leprosy and multiple myeloma. Table 2.1

Drugs proposed for chemoprevention and treatment of skin cancer	22
Table 2.2 Summary of flavonoids used in the treatment of melanomas with mechanism of actions	24
Table 2.3 Physicochemical properties of DHA.....	26
Table 2.4 Role of DHA in the treatment of melanoma	28
Table 2.5 Physicochemical properties of HES.....	30
Table 2.6 Studies on hesperidin and its formulation in melanoma therapy	33
Table 2.7 Summary of different drug loading methods into exosomes	42
Table 4.1 List of materials used in the experiments and their sources	47
Table 4.2 List of instruments used in the experiments and their sources.....	50
Table 4.3 List of software used	52
Table 5.1 HPLC parameters for DHA method development and validation	57
Table 5.2 HPLC parameters for DHA method development and validation for <i>in vivo</i> analysis	59
Table 5.3 Different levels and constraints for variables in BBD	62
Table 5.4 The runs obtained from the Box Behnken Design	63
Table 5.5 Accuracy studies of the developed HPLC method for DHA (n=3).....	77
Table 5.6 Repeatability study of HES-developed HPLC method (n=8).....	77
Table 5.7 Intermediate precision (Intra-day and inter-day precision) studies of the DHA-developed HPLC method.....	77
Table 5.8 Robustness and ruggedness study of developed HPLC method for DHA (10 µg/ml)	78
Table 5.9 Accuracy studies of the developed HPLC method for DHA (n=3).....	80
Table 5.10 Repeatability study of HES-developed HPLC method (n=8).....	80
Table 5.11 Intermediate precision (Intra-day and inter-day precision) studies of the DHA-developed HPLC method.....	81
Table 5.12 Robustness and ruggedness study of developed HPLC method for DHA (10 µg/ml).....	82
Table 5.13 Particle size, PDI, zeta potential, encapsulation efficiency, and drug loading of exosomes and DHA-loaded exosomes.....	84
Table 5.14 BBD with independent variables (factors) and the experimental response for the process optimization	85
Table 5.15 Analysis of Variance (ANOVA) testing results of the models	85
Table 5.16 Pharmacokinetic parameters of DHA and Exo-DHA after oral administration...	103
Table 5.17 Evaluation of blood parameters after completion of the treatment period.....	107
Table 6.1 HPLC method parameters for HES.....	114
Table 6.2 HPLC parameters for HES method development and validation for <i>in vivo</i> analysis	117

Table 6.3 Accuracy studies of the developed HPLC method for HES (n=3)	129
Table 6.4 Repeatability study of HES-developed HPLC method (n=8).....	129
Table 6.5 Intermediate precision (Intra-day and inter-day precision) studies of the HES-developed HPLC method.....	129
Robustness measures the HPLC technique’s resistance to small, deliberate changes in method variables, indicating its reliability under typical operating conditions. Table 6.6 Robustness and ruggedness study of developed HPLC method for HES (10 µg/ml).....	130
Table 6.7 Accuracy studies of the developed HPLC method for HES (n=3)	132
Table 6.8 Repeatability study of HES-developed HPLC method (n=8).....	133
Table 6.9 Intermediate precision (Intra-day and inter-day precision) studies of the HES-developed HPLC method.....	133
Table 6.10 Robustness and ruggedness study of developed HPLC method for HES (10 µg/ml)	134
Table 6.11 Particle size, PDI, zeta potential, encapsulation efficiency, and drug loading of exosomes and HES-loaded exosomes.....	135

List of Abbreviations

Abbreviations	Description
2FI	Two-factor interaction model
ABC	ATP-binding cassette
ABCD	Asymmetry, border irregularity, color variation, and large diameter
AFM	Atomic force microscope
Akt	Ak strain transforming kinase
ALP	Alkaline phosphatase
ANOVA	Analysis of variance
AP-1	Activated protein-1
AT	Artemisinin
AUC	Area under the curve
b.wt	Body weight
BBB	Blood-brain barrier
BCC	Basal-cell carcinoma
BM	Branching myocytes
BRAF	Serine/threonine-protein kinase B-Rapidly Accelerated Fibrosarcoma
C.V.	Co-efficient of variation
CCD	Central composite design
CDER	Center for Drug Evaluation and Research
CDK4	Cyclin-dependent kinase 4
CDKN1A	Cyclin-dependent kinase inhibitor 1A
CDKN2A	Cyclin-dependent kinase inhibitor 2A
CLSM	Confocal laser scanning microscopy
CM	Cutaneous melanoma

C _{max}	Maximum plasma concentration
COX-2	Cyclooxygenase 2
CPCSEA	Committee for the Purpose of Control and Supervision of Experiments on Animals
CQA	Critical quality attributes
CREB	Cyclic AMP response element-binding protein
CTLA-4	Cytotoxic T-lymphocyte-associated antigen 4
CU-6	Cumarin-6
DAD	Diode array detector
DHA	Dihydroartemisinin
DM	Desmoplastic melanoma
DMBA	Dimethylbenz[a]anthracene
DMEM	Dulbecco's Modified Eagle's Medium
DMSO	Dimethylsulphoxide
dNTPs	Deoxynucleoside triphosphate
DTIC	Dacarbazine
ECL	Enhanced Chemiluminescence
EE	Encapsulation efficiency
EGF	Epidermal growth factor
EGFR	Epidermal growth factor receptor
ERK1/2	Extracellular signal-regulated kinases 1 and 2
ESCRT	Endosomal sorting complexes required for the transport
EVs	Extracellular vesicles
Exo	Exosomes
Exo-C-6	Exosomes loaded coumarin-6
Exo-DHA	Dihydroartemisinin loaded exosomes
Exo-HES	Hesperidin loaded exosomes

FbD	Formulation by design
FBS	Fetal bovine serum
FDA	Food and Drug Administration
FGF	Fibroblast growth factor
FGFR	Fibroblast growth factor receptor
F _{rel}	Relative bioavailability
GCO	Global Cancer Observatory
GEM	Genetically engineered models
GGT	γ -glutamyl transpeptidase
GHS	Globally Harmonised System
GM-CSF	Granulocyte-macrophage colony-stimulating factor
GSH	Glutathione
GTP	Guanosine triphosphate
HEK 293	Human embryonic kidney 293 cells
HES	Hesperidin
HIF-1 α	Hypoxia-inducible factor-1 α
HPLC	High-performance liquid chromatography
HRAS	Harvey rat sarcoma viral oncogene homolog
HRSEM	High-resolution scanning electron microscopy
HRTEM	High-resolution transmission electron microscopy
i.p.	Intra peritoneal
iNOS	Inducible nitric oxide synthase
IAEC	Institutional Animal Ethics Committee
ICH	International Conference on Harmonization
IFN	Interferon
IL	Interleukin

ILVs	Intraluminal vesicles
K_0	Zero order rate constant
K_1	1 st order rate constant
KDR/Flk-1	Kinase insert domain receptor/fetal liver kinase 1
K_{el}	Elimination rate constant
LD ₅₀	Lethal Dose 50
LOD	Lower limit of detection
LOQ	Lower limit of quantification
LMM	Lentigo maligna melanoma
LOD	Limit of detection
LOQ	Limit of quantification
MAPK	Mitogen-activated protein kinase
MCWO	Molecular weight cutoff
MEK	Mitogen-activated protein kinase kinase
MEK1/2	MAP kinase extracellular signal regulated kinases 1 and 2
MHC	Major histocompatibility complex
MMP	Mitochondrial membrane potential
MMPs	Matrix metalloproteinases
MRT	Mean residence time
MVBs	Multivesicular bodies
NCCS	National Centre for Cell Science
NCEs	New chemical entities
NCI	National Cancer Institute
NF- $\kappa\beta$	Nuclear factor kappa β
NK	Natural killers
NRAS	Neuroblastoma RAS viral oncogene homolog

OECD	Organization for Economic Co-operation and Development
p.o.	Per oral
PBS	Phosphate-buffered saline
PCNA	Proliferating cell nuclear antigen
PD-1	Programmed cell death protein 1
PD-L1	Programmed cell death ligand 1
p-DMAB	p-dimethylaminobenzaldehyde
PDTXs	Patient-derived tumor xenografts
P-gp	P-glycoprotein
PI3K	Phosphatidylinositol-3-kinase
PIP2	Phosphatidylinositol- 4, 5-biphosphate
PIP3	Phosphatidylinositol-3, 4, 5-triphosphate
PK	Pharmacokinetic
PKC α	Protein kinase C alpha
PLGA	Poly(lactic-co-glycolic acid)
QbD	Quality by design
QC	Quality control
Raf	Rapidly accelerated fibrosarcoma
Ras	Rat sarcoma virus
RDW	Red cell distribution width
RET	Receptor tyrosine kinase
RES	Reticuloendothelial system
ROS	Reactive oxygen species
RSD	Relative standard deviation
Rt	Retention time
RTK	Receptor tyrosine kinase

SCC	Squamous cell carcinoma
SCID	Severe combined immune-deficient
SD	Standard deviation
SEC	Size exclusion chromatography
SPM	Scanning probe microscopy
$t_{1/2}$	Elimination half-life
TCR	T-cell receptor
TDDS	Transdermal drug delivery system
TGF	Transforming growth factor
TGI	Tumor growth inhibition
TIMP	Tissue Inhibitor of Metalloprotease
TLC	Total leucocyte count
T_{max}	Time to reach maximum concentration
TMF	5,7,4'trimethoxyflavone
TNF	Tumor necrosis factor
TRBCs	Total red blood cell counts
TV	Tumor volume
UV	Ultraviolet
VDT	Volume doubling time
VEGF	Vascular endothelial growth factor
VPS4	Vacuolar protein sorting associate protein 4
WBC	White blood cells
XRD	X-ray diffraction

List of Symbols

Symbols	Description
%	Percentage
°	Degree
α	Alpha
μ	Micro
β	Beta
γ	Gamma
μg	Microgram
mm	Milli meter
cm	Centi meter
>	Greater than
<	Less than
↑	Increase
↓	Decrease
°C	Degree Celsius
T_g	Glass transition temperature
MW	Molecular weight
®	Registered trademark
TM	Trademark
μL	Micro liter
mAU	Milli-absorbance unit
ppm	Parts per million
v	Volume
nm	Nano meter

λ_{\max}	Absorption maxima
bp	Base pair
kH	Kilohertz
W	Watt
min	Minute
#	Mesh size
rpm	Rotation per minute
θ	Theta
g	Gram
mg	Milli gram
cm	Centi meter
w	Weight
s	Second
h	Hour
ζ	Zeta potential
mV	Milli volt
mg/dL	Milligram/deciliter
U/L	Unit/liter
g/dL	Gram/deciliter
fL	Femtoliters
pg	Picogram